INTERNATIONAL JOURNAL OF AUTOMOTIVE AND MECHANICAL ENGINEERING (IJAME)
ISSN: 2229-8649 e-ISSN: 2180-1606
VOL. XX, ISSUE XX, XXX – XXX
DOI: https://doi.org/10.15282/ijame.v#i#.###

ORIGINAL ARTICLE

Fully-Coupled Modelling and Experimental Validation of Quarter Wavelength Resonator with Piezoelectric Backplate in Vibro - Acoustic Energy Harvesting

Muhammad Hatifi Mansor[1]*, Mohd Shahrir Mohd Sani[1], Mohd Firdaus Hassan[1] and Lihua Tang[2]

[1]Faculty of Mechanical and Automotive Engineering Technology, Universiti Malaysia Pahang Al-Sultan Abdullah, Pekan 26600 Pahang, Malaysia
[2]Department of Mechanical Engineering, University of Auckland, Auckland, New Zealand

ABSTRACT – Converting and harvesting the unwanted sounds produced by noise, especially in busy cities, can solve the issue of sound pollution and provide renewable power sources for low-power electronics. Although sound energy is freely available, it is hard to harvest due to its relatively low energy density compared to other sources. To enhance the efficiency of acoustic energy harvesting, particularly in the low-frequency range. The intgration of an optimised resonator is essential. This research study explores the performance of a vibroacoustic energy harvester incorporating a straight tube quarter-wavelength resonator coupled with a piezoelectric patch mounted on a flexible backplate. A fully coupled finite element model (FEM) was developed to capture the interaction between acoustic field, structural dynamic and piezoelectric transduction, and its predictions were validated against experimental results. The numerical model yielded a maximum output voltage of 1.41 V/Pa at 112 Hz, closely matching experiment findings of 1.44 V/Pa at 106 Hz under an incident sound pressure level of 90 dB. The proposed modelling framework demonstrates strong predictive capability and provides a robust basis for the design and optimisation of low-frequency acoustic energy harvester based on quarter-wavelength resonator configuration.

ARTICLE HISTORY
Received: xxxx
Revised: xxxx
Accepted: xxxx
Published: xxxx

KEYWORDS
Fully-coupled
Vibro-Acoustic
Energy Harvesting
Piezoelectric

1.0 INTRODUCTION

Sound energy, as a manifestation of mechanical vibrational energy, represents a clean and environmentally sustainable alternative for powering low-power electronic devices or systems [1,2]. Although the overall energy conversion efficiency of acoustic energy harvesting (AEH) remains relatively modest and several practical challenges persist, the pervasiveness of ambient sound in everyday environments and its negligible ecological footprint has spurred growing interest in this approach [3]. AEH systems are typically composed of an acoustic resonator coupled with electromechanical transducers such as piezoelectric or electromagnetic elements that facilitate the conversion of sound energy into electrical output. A range of resonator geometries has been explored to enhance energy harvesting performance, including Helmholtz resonators [4,7], quarter-wavelength resonators (QWRs) [6], deep-subwavelength devices [5], and sonic crystals [8]. These configurations are designed to amplify sound pressure levels at designated frequencies, thereby increasing transduction efficiency [9]. Despite notable advancements, two critical limitations remain. First, much of the prior research has centred on high-frequency AEH devices, whereas low-frequency sound sources are more commonly encountered in practical settings due to their reduced attenuation over distance and broader spatial coverage [15,16]. Second, many modelling approaches employed in existing studies rely on a decoupled treatment of the acoustic and structural domains, neglecting the intricate electromechanical coupling that plays a vital role in determining the overall system response [17–20]. This decoupling can lead to inaccurate predictions of device performance and hinder the effective design and optimisation of AEH systems.

Recent research has pushed the boundaries of acoustic energy harvesting (AEH) by investigating hybrid resonator configurations and novel piezoelectric integration techniques. Xiao et al. [21] demonstrated that metamaterial-enhanced piezoelectric harvesters could achieve significantly higher efficiency due to localised resonance effects, but their effectiveness is still constrained in low-frequency domains (<200 Hz) where energy density remains low. Pushpa and Kumar [22] reviewed optimisation strategies for AEH systems, emphasising that impedance matching and dynamic tuning of the resonator–piezo interface is crucial for real-world deployment. However, most optimisation studies focus on simplified, decoupled models, which may fail to capture the nonlinear interactions and back-coupling effects between acoustic pressure fields and piezoelectric elements in integrated systems. Other recent advancements have focused on developing analytical and semi-analytical tools for improving design accuracy and simulation speed. Islam et al. [23] introduced a hybrid modelling framework combining Green's function approaches with finite element analysis to enable rapid design iterations in low-frequency AEH systems. While promising, such methods still rely on simplifying assumptions regarding boundary conditions and structural–acoustic coupling. Alshahrani et al. [24] proposed impedance-

*CORRESPONDING AUTHOR | M.H. Mansor | ✉ hatifi@umpsa.edu.my

matching layers for acoustic resonators to enhance wave transmission into the harvester structure, showing improved voltage gains of up to 40% in experimental settings. Yet, these studies have largely neglected the synergistic dynamics between structural deformation, acoustic feedback, and electrical load in fully coupled systems.

Despite these developments, a persistent challenge remains in accurately predicting the behaviour of integrated AEH systems where structural, acoustic, and electrical fields interact nonlinearly. Most prior studies have either limited themselves to static boundary conditions or omitted experimental validation entirely. While quarter-wavelength resonators (QWRs) are well known for their low-frequency amplification characteristics, few investigations have examined the design implications of flexible backplates embedded with piezoelectric patches. This work addresses these limitations by developing a fully coupled finite element model validated through experimentation, providing a comprehensive design methodology for optimised QWR-based AEH technologies.

To address these challenges, the present study develops and validates a fully coupled vibroacoustic energy harvesting model based on a quarter-wavelength resonator with a piezoelectric (PZT) backplate. The system is designed to synchronise the mechanical resonance of the PZT transducer with the acoustic resonance of the QWR, enhancing energy transfer and conversion efficiency. A finite element model is developed to capture the coupled interaction between the acoustic field and the structural response, and the simulation results are validated experimentally using a vertical QWR tube subjected to acoustic excitation ranging from 50 Hz to 300 Hz at approximately 90 dB. The theoretical resonance frequency of the QWR is estimated at 117 Hz. This study aims to advance the understanding of fully coupled AEH systems and contribute to the design of efficient low-frequency acoustic energy harvesting technologies.

2.0 THE PRINCIPLE OF WORK QUARTER WAVELENGTH RESONATOR

Depending on its size, a resonator tube is a device made up of parts arranged so that their acoustic reactance is neutralised at a specific frequency. An acoustic system is commonly used as a passive way to eliminate unwanted frequency components or control sound. At its resonance frequency, the acoustic resonator tube can also raise the acoustic pressure [25].

Two well-known resonators that have been thoroughly researched for acoustic applications are the quarter-wavelength and Helmholtz resonators [26]. Recently, a third kind of resonator, a half-wavelength resonator, has been developed to offer acoustic dampening [26, 27]. Chae et al. [26] used a half-wavelength resonator as a baseline to compare the efficacy of these three resonators. According to the evaluations, a quarter-wavelength resonator offered the maximum acoustic energy harvesting efficiency compared to the other two resonators [18]. Neither straight tube resonator could be modelled using lumped elements like the HR resonator, since the longitudinal component's length is equivalent to the wavelength. The linear resonator's two lengths regulated the fundamental frequencies. The sound pressure propagating into a stiff quarter-wavelength resonator tube is depicted in **Figure 1.**

Harmonic plane waves are a fundamental concept in wave propagation and have various applications, including resonators with embedded piezoelectric transducers. In the case of a quarter-wavelength resonator with a fixed thin circular backplate embedded piezoelectric transducer, the harmonic plane wave propagation derivation involves several key steps. The wave equation describes the propagation of acoustic waves in a medium. In one dimension for an acoustic wave in air, the wave equation is given by [28]

$$\frac{\partial^2 p(z,t)}{\partial t^2} = C^2 \frac{\partial^2 p(z,t)}{\partial z^2} \tag{1}$$

where $p(z,t)$ is the acoustic pressure as a function of position z along the resonator and time t. C is the speed of sound in the medium. The general equation for plane wave propagation in a medium is used, which states that the displacement field can be represented as a product of a harmonic plane wave and a spatial profile function. When the wavelength in the medium is much longer than the dimensions of the tubes, the analysis of many acoustic tubes becomes modest. A rigid quarter-wavelength resonator tube's inlet is shown in **Figure 1** with a harmonic sound pressure solution for p,z, and$t$ applied. The sound pressure propagates in the z-direction, as shown in [1, 28].

$$\left.\begin{aligned} p(z) &= P_i e^{-ikz} e^{i\omega t} \\ u(z) &= \frac{P_i}{\rho_0 c} e^{-ikz} e^{i\omega t} \end{aligned}\right\} for\ z > 0 \tag{2}$$

$$\left.\begin{aligned} p(z) &= P_r e^{ikz} e^{i\omega t} \\ u(z) &= \frac{P_r}{\rho_0 c} e^{ikz} e^{i\omega t} \end{aligned}\right\} for\ z < 0 \tag{3}$$

where p and u are the pressure and velocity of the air in the tube with the L length, ρ_0 is the equilibrium air density; $k = {}^{\omega}/_{c_0}$ is the wavenumber and c_0 is the wave speed. It is noted that both are complex amplitudes. Based on **Figure 1**, the boundary condition at z is equal to 0 and the equations (2) and (3) become:

$$P_r = P_0 - P_i \tag{4}$$

Equation (4) defines the relationship between reflected pressure, P_r, and the difference between the pressure at the inlet and the incident pressure, P_i. For the second boundary condition, the backplate was rigid. By substituting equation (2) into equation (4), the particle velocity of sound pressure at z equal to L is 0, and the final equation becomes

$$P(z) = \left(\frac{P_0 e^{ikL}}{(e^{-ikL}+e^{ikL})}\right) e^{-ikz} + \left(P_0 \frac{P_0 e^{ikL}}{(e^{-ikL}+e^{ikL})}\right) e^{ikz} \tag{5}$$

The equation (5) calculates the overall acoustic pressure within the quarter wavelength tube when a rigid backplate is present. Based on this equation, Bin Li et al. [20] determined a suitable site to install the PVDF within the quarter wavelength resonator. This operation substantially impacted the value of the standing wave and eigenfrequency in the quarter wavelength tube. A flexible backplate was used instead of a solid backplate to keep the two critical parameters stable. The backplate is designed to be flexible and includes a piezoelectric patch. This patch uses the acoustic pressure and air particle velocity that occur naturally within the resonator tube. At the end of the resonator, the velocity of air particles matches the velocity of a flexible backplate rather than being zero when a rigid backplate is employed.

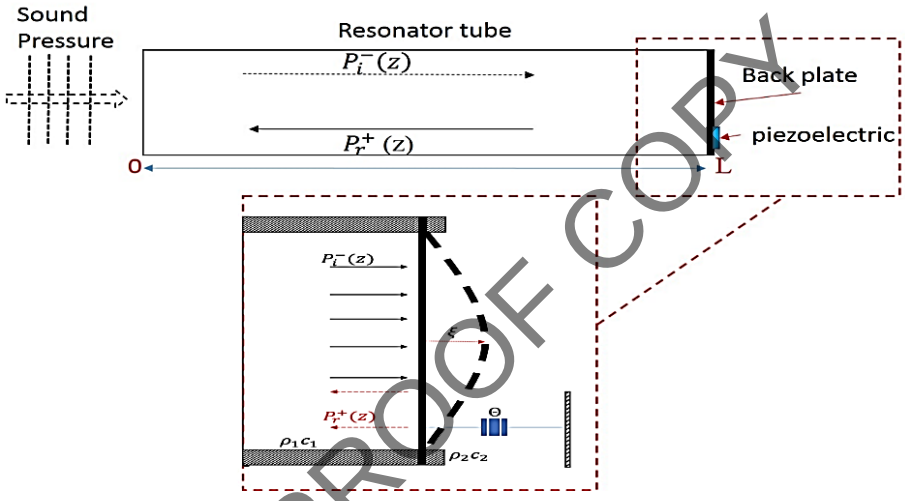

Figure 1. A quarter-wavelength resonator tube's L length experienced a sound pressure reflected at the flexible backplate.

The equilibrium air density inside the tube is represented by the medium ρ_1 and the speed sound c_1, while the medium ρ_2 and the speed sound c_2 represent the air density on the opposite side of the backplate. **Figure 1** shows a harmonic sound pressure equation (2) that was applied at the inlet of the quarter-wavelength resonator tube and reflected. Boundary condition similar to equation (5) at the z = 0 and the coefficients P_i *and* P_r is linked by the average particle velocity at the left-hand of the backplate inside the tube, which moves with an average velocity equal to $j\omega\xi$. On the other end, when z = L, the acoustic pressure field in the negative z-direction by displacement ξ is given by

$$P_i e^{-ikL} - P_r e^{ikL} = j\omega\xi\rho_1 c_1 \tag{6}$$

while the total pressure field in the resonator tube is given by

$$P^-(z) = P_i e^{-ikz} e^{i\omega t} + (P_0 - P_i) e^{ikz} e^{i\omega t} \tag{7}$$

The incidence and reflection from a complete QWR backplate produced the first equation (7) term, which represents the standing interference field. The second term describes the pressure field produced by backplate motion. Therefore, the total area on the incident side equals the sum of the radiated field and the pressure field produced by the backplate. The radiated field, which is represented by the backplate displacement is therefore, the only field on the right-hand side, expressed as

$$\xi(r,t) = \xi \cos(\omega t) J_0 \left(\frac{\pi r}{R}\right) \tag{8}$$

where ξ is the amplitude of the displacement, R is the radius of the circular backplate, and J_0 is the first kind of zeroth-order Bessel function. In order to account for the impact of the backplate, equation (8) incorporates the equation of motion for the backplate, which establishes a connection between the displacement of the backplate and the gradient of the acoustic pressure from equation (7). This equation accounts for the density and stiffness of the backplate material.

The piezoelectric effect introduces the piezoelectric strain, which is directly linked to the mechanical strain by means of the piezoelectric coefficient. The piezoelectric strain equation is then given by

$$\varepsilon(r,t) = d_{31}\frac{\partial \xi(r,t)}{\partial r} \tag{9}$$

Equation (9) is related to the radial displacement of equation (10) of the backplate. The piezoelectric strain coefficient d_{31} links the mechanical deformation to the electrical response in the material and the piezoelectric strain $\varepsilon(r,t)$ in the backplate is:

$$\varepsilon(r,t) = d_{31}\frac{\pi\xi}{R}\sin(\omega t)J_1\left(\frac{\pi r}{R}\right) \tag{10}$$

where J_1 is the first-order Bessel function of the first kind. Charge distribution is obtained by integrating the piezoelectric strain over the area of the circular backplate, thus resulting

$$Q(r,t) = \int_0^{2\pi}\int_0^R \varepsilon(r,t)r\,dr\,d\theta \tag{11}$$

The piezoelectric effect generates electric potential or voltage in response to applied mechanical stress. In the case of the embedded piezoelectric transducer, the transducer converts the mechanical wave into an electrical signal. This phenomenon is achieved through the interaction between the electric field $E(r,t)$ across the piezoelectric transducer, which is related to the charge through capacitance C, given by

$$C\frac{\partial E(r,t)}{\partial t} = Q(r,t) \tag{12}$$

Equation (12) states that the rate of change of the electric field, multiplied by the capacitance, is equal to the charge produced in the piezoelectric material due to mechanical stress. When converting signals to the frequency domain to analyse harmonic components, the relationship between the signals becomes more straightforward. The electric field is present in this location, written as

$$E(r,\omega) = \frac{Q(r,\omega)}{C} \tag{13}$$

Equation (13) indicates that the ratio of the charge to the capacitance determines the electric field in the frequency domain. For a harmonic excitation with angular frequency ω the second time derivative of the electric field $E(r,t)$ is related to the piezoelectric coefficient, the strain amplitude, and the spatial integration involving the Bessel function. The equation can be expressed as

$$C\frac{\partial^2 E(r,t)}{\partial t^2} = -2\pi d_{31}\xi\cos(\omega t)\int_0^R rJ_1\left(\frac{\pi r}{R}\right)dr \tag{14}$$

This equation describes how a piezoelectric transducer turns mechanical vibrations into an electrical signal. The electric field, charge, and capacitance were related in both the time and frequency domains. The dynamic connection also considers the system's mechanical strain and spatial properties, resulting in a thorough mathematical model of the piezoelectric effect in the resonator.

The acoustic pressure (in equation (2)) is related to the backplate motion $z = \frac{2r}{\pi}$ through spatial coordinate transformation, thus resulting in equation (15), where

$$P(z,t) = P_0\cos\left(\omega t - k\frac{2r}{\pi} + \emptyset\right) \tag{15}$$

Combining the expressions for the acoustic pressure and the electric field will create a coupled equation that describes the interaction between the acoustic wave and the piezoelectric transducer, given by

$$C\frac{\partial^2 E(r,t)}{\partial t^2} = -2\pi d_{31}\xi\cos(\omega t)\int_0^R \frac{z\pi}{2}J_1\left(\frac{\pi r}{R}\right)dr \tag{16}$$

The dispersion relationship characterises the relationship between a wave's frequency and wave number, determining how a harmonic plane wave travels in a resonator with a piezoelectric transducer [28]. The derived dispersion relations serve as a fundamental tool for analysing and enhancing the performance of acoustic resonators, enabling the determination of key parameters such as resonant frequencies and mode shapes [29]. A clear understanding of how sound waves travel through a resonator allows for the development of precise models and simulations. These tools are essential for designing more effective resonators and enhancing their performance across a range of operating conditions, particularly in acoustic energy harvesting applications.

3.0 METHODOLOGY

3.1 Finite Element Analysis of Vibro-Acoustic Energy Harvesting

A three-dimensional, fully coupled model of the proposed acoustic energy harvester was developed in this work using

the commercial finite element (FE) tool. One challenging multiphysics topic that can be solved with numerical methods is the study of acoustic energy harvesting. Discretising the resonator and piezoelectric into a mesh of elements can solve the governing equations for acoustic waves and piezoelectric constitutive relations in tandem. First, a harmonic acoustic analysis determines the pressure distributions and resonance frequencies of quarter-wavelength standing waves in the cylindrical cavity. The amplification effects of resonances are quantified. Next, the mechanical strains imposed on the piezoelectric element by resonant acoustic waves are estimated using equations that relate pressure gradients to solid surface displacements. Circuit equations then connect the electrical outputs of the strained piezoelectric material to a connected harvesting circuit. The load resistance is optimised to maximise power output at a given input pressure level. The fluid-structure interaction and the electromechanical link were taken into consideration in the model. This study examines the theoretical equations through simulation and experimental verification.

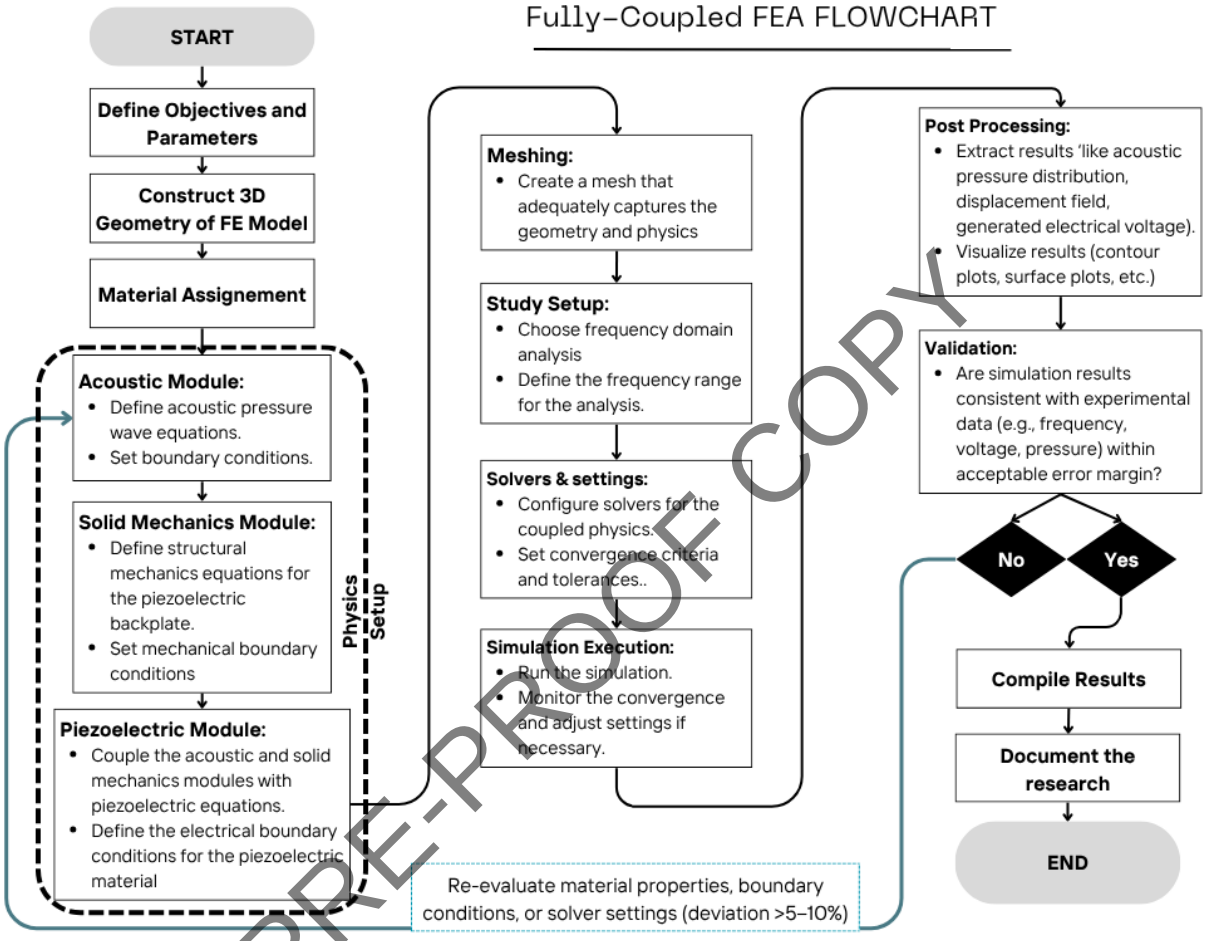

Figure 2. Fully-coupled finite element analysis, Multiphysics AEH system flowchart

This work involved a comprehensive analysis of low-frequency acoustic energy harvesting. From **Figure 2,** the COMSOL Multiphysics software was used to analyse a quarter-wavelength resonator with a piezoelectric backplate. The process consisted of three crucial parts. The study began by identifying the target frequency range (low-frequency) and specifying all relevant material properties, including piezoelectric constants and mechanical characteristics. A detailed geometry of the quarter-wavelength resonator was then created, incorporating the piezoelectric backplate, with appropriate materials assigned to each part. Using COMSOL Multiphysics, the model integrated acoustic, structural, and piezoelectric physics. This was achieved by employing the Acoustic Module for pressure wave analysis, the Solid Mechanics Module for structural response, and the Piezoelectric Module to couple mechanical and electrical fields.

Mesh generation was carefully performed, with refinement near interfaces to ensure accurate results. A frequency domain study was chosen to examine the system's response across a range of frequencies. Solver settings were adjusted according to the model's size and complexity, using either direct or iterative methods as appropriate. The simulation results focused on acoustic pressure distribution, structural deformation, and the resulting electrical output. These results were validated through comparison with experimental data to ensure accuracy and reliability. Where necessary, optimisation was carried out to improve model performance. The following section presents a detailed discussion of the fully coupled finite element analysis used in this research.

3.1.1 Geometry of quarter wavelength resonator (QWR)

The finite element model of the QWR with a PZT backplate is built in COMSOL. The setup for the model environment must be determined first before constructing the model's geometry. At this stage, the model will decide whether to build the geometry in 2D or 3D. Then, the geometry tool will be used inside the software to build the cylinder shape of an open-closed straight tube, where the closed end will be embedded with the piezoelectric transducer patch. A piezoelectric transducer bond is used to clamp the piezoelectric backplate circumferentially. After that, two spherical pieces that make up an air domain are constructed outside the QWR. One Pascal, an acoustic plane wave, is produced as a sound source by the tiny spherical region outside the resonator.

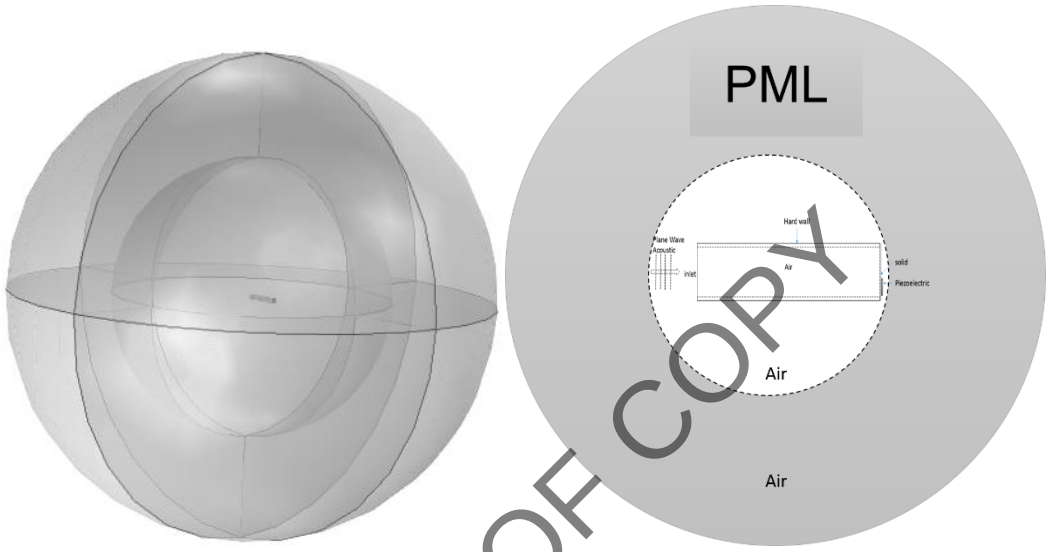

Figure 3. Fully connected finite model element: (a) a three-dimensional model comprising a quarter-wavelength resonator, plane wave source domain, and PML domain (b) a 2D model that depicts a 3D model part.

In contrast, the larger spherical domain outside the QWR and the first spherical air domain is the perfectly matched layer (PML). Two- and three-dimensional representations of the system are displayed in **Figure 3** as part of the primary component. The larger spherical diameter size of the PML is up to three wavelengths of the QWR model, and the acoustic plane wave spherical diameter size is one wavelength of the QWR model. The QWR tube is within a global computational domain with a total radius of four wavelengths at 117 Hz. Three wavelengths make up the thickness of the perfect match layer. In modelling the acoustic domain, appropriate boundary conditions are essential for accurately capturing wave propagation and resonance effects. This study employs the Perfectly Matched Layer (PML) technique to simulate wave absorption at the open end of the quarter-wavelength resonator (QWR). The PML is implemented as an anisotropic absorbing layer that minimises reflections from the domain boundary, effectively emulating an open or infinite domain.

Although alternatives such as Plane Wave Radiation (PWR) and Simple Boundary Conditions (SBCs) are commonly used in acoustic modelling, they have limitations in scenarios involving low-frequency resonance and broadband acoustic excitation, as in the current study. PWR, for instance, assumes a dominant plane wave propagation mode and is less effective when higher-order modes or structural-acoustic coupling are present. SBCs lead to unphysical reflections and distorted pressure fields. The choice of PML ensures improved accuracy in modelling the standing wave patterns and acoustic energy transmission within the QWR, especially under fully coupled simulation conditions. A comparison of the three boundary condition methods used in this research is provided in **Table 1**.

Table 1: Comparative Summary of Acoustic Boundary Condition Techniques

Boundary Condition	Key Characteristics	Advantages	Limitations
Perfectly Matched Layer (PML)	Absorbs outgoing waves with minimal reflection	Highly accurate; suitable for broadband signals	Requires careful tuning; more computationally intensive
Plane Wave Radiation (PWR)	Assumes plane wave propagation at boundaries	Efficient, simple to implement	Limited accuracy for complex or low-frequency modes

Simple Boundary Conditions (SBCs)	Basic acoustic boundary (e.g., rigid or impedance wall)	Computationally cheap	High reflection, poor physical realism

Future studies will explore the influence of boundary condition variations on resonance behaviour and energy conversion efficiency using a systematic parametric analysis.

3.1.2 Material properties and boundary conditions

Material properties are characteristics that describe material behaviour mathematically, usually through coefficients and constitutive equations. In the FEM, the material properties of each element and the geometric parameters of the three-dimensional model for finite element analysis are listed in **Table 2**. The QWR will be known as acrylic and hard wall with backplate properties such as Young's modulus, Poisson's ratio and density. The piezoelectric patch geometric and material properties also will be defined in the FEM software before meshing setup.

Table 2: Geometric and material properties of the AEH system

Parameters	**Value**
QWR tube:	
Diameter	100 mm
Length	735 mm
Wall Thickness	5 mm
Backplate:	
Diameter	100mm
Thickness	4 mm
Backplate Properties:	
Young Modulus (E)	0.84 – 1 GPa
Poisson's Ratio	0.35
Density (ρ)	1190 kg/m^3
Piezoelectric patch transducer:	
Length	37 mm
Width	18 mm
Thickness	0.5 mm
Piezoelectric capacitance (c_p)	30.78 nF
Piezoelectric density (ρ_p)	7750 kg/m^3
Piezoelectric Young's Modulus (E_p)	30.36 GPa
Piezoelectric Relative permittivity	
$\varepsilon_{33}/\varepsilon_0$	1750
$\varepsilon_{11}/\varepsilon_0$	1650
Piezoelectric charge coefficient	
d_{31}	-180
d_{33}	400
Room Temperature	15 °C
Density	1.2250 kg/m^3
Sound of Speed (c_0)	340.27 m/s

An absorbing and non-reflective border was used as the PML's boundary condition. PML depicts sound radiation in an infinite domain, so it was chosen despite the higher memory and computing expenses. Only outgoing waves are permitted by the PML's particular radiation boundary condition and huge spherical component, as seen in **Figure 3(b)**. Air constituted the surrounding fluids for this global domain. Through the resonator inlet, acoustic plane waves are produced and transmitted inside the QWR tube, occupying the second spherical domain. Radiation from the plane wave outside the QWR will enter the PML layer. The plane wave introduced in the second spherical domain will coincide with the incident wave from the intake inside the resonator tube after reflecting at the flexible backplate.

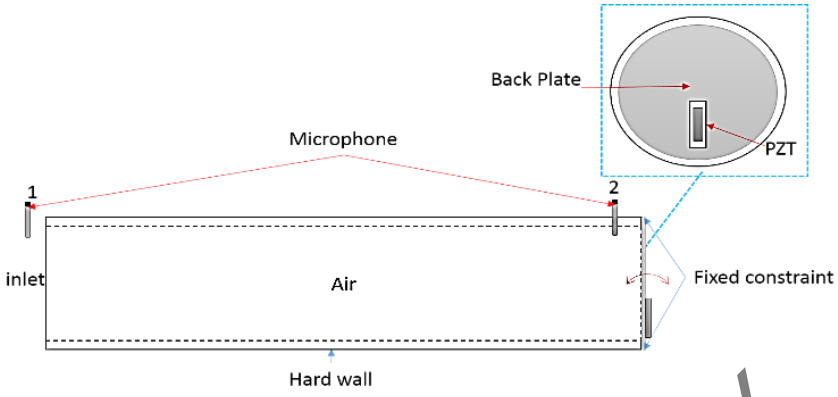

Figure 4: Acoustic structure piezoelectric interaction boundary requirement for AEHs

The flexible QWR backplate measures 10 cm in diameter and is 4 mm thick, with an acrylic construction. It is fastened to the QWR tube's closed end at the circular edge. The most substantial movement was induced by a piezoelectric device constructed of Lead Zirconate Titanate (PZT-5) placed on the backplate in that position. **Figure 4** indicates the model's configuration. In order to replicate electrodes, the electrical boundary condition linked the piezo's top and bottom surface voltage degrees of freedom. One side of the piezoelectric is grounded, while the other is an open circuit. This boundary condition will result in the open-circuit voltage of the output (VOC). After that, the resistive load was positioned on the open circuit surface to produce the best power output and voltage close circuit. The first microphone recorded the acoustic pressure at the inlet, where the incident wave occurs. The second microphone measured the acoustic pressure at the end of the resonator, where the standing wave would appear. The rigid construction of the resonator is shown in **Figure 4**, where the flexible acrylic backplate functions as a structure that engages with the acoustic domain.

In conclusion, material qualities measure a material's capacity and usefulness. Comprehending these crucial characteristics for the application's operating conditions while selecting materials and estimating performance is essential.

3.1.3 Mesh and solver

The meshing in the FEM is a mathematical representation of a physical domain divided into small components known as elements [30] also known as a mathematical discretisation of a physical domain where all the domains starting from the PML layer, acoustic wave source layer and quarter wavelength resonator had been visually broken down into a collection of smaller inter-connected pieces. Typical elements used for discretising the domain are tetrahedral shapes in 3D.

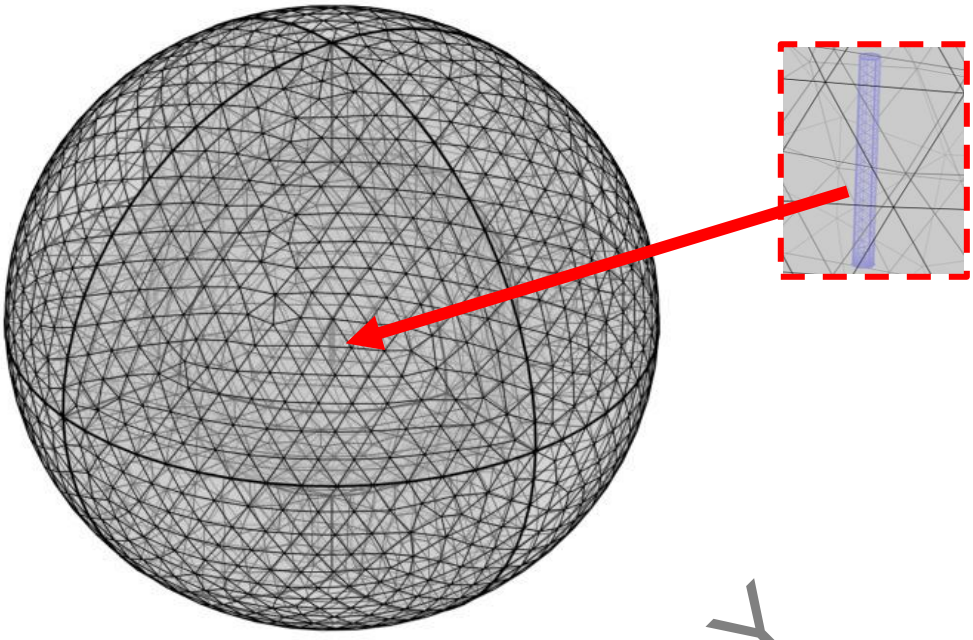

Figure 5: FEM mesh model of quarter wavelength resonator in the PML domain

The meshing component of acoustic energy harvesting with a quarter-wavelength resonator is depicted in **Figure 5**. As displayed above, the final mesh has 102935 tetrahedra and 8635 triangle elements. Even in parts of geometry where far fewer elements would be sufficient for meshing, this number of elements resolves the geometry rather well, lowering the memory needs. The mesh inside the perfectly matched layer (PML) was also required for mesh maintenance. To properly attenuate the outward waves, it is recommended that the PML utilise a sweeping mesh with six components. Meshing is essential to get a better outcome in the shortest simulation time.

When modelling a wave problem, the computational mesh must sufficiently resolve the waves. This 3D acoustic model requires a minimum of 6 components per wavelength when employing second-order elements, typically used in pressure acoustics. The acoustic model restricts the mesh's maximum element size to

$$L_{max} = \frac{\lambda_0}{6} \tag{17}$$

Precise design of solvers and settings is essential in the fully coupled study of low-frequency acoustic energy harvesting employing a quarter-wavelength resonator fitted with a piezoelectric backplate in COMSOL software to ensure correct findings. This study utilised a frequency domain analysis to examine the system's reaction within a designated frequency spectrum. A completely integrated solver technique managed the interplay between acoustic, structural, and piezoelectric fields. The selection of direct solvers, such as MUMPS (MUltifrontal Massively Parallel Sparse Direct Solver), was based on their ability to handle strongly coupled and potentially ill-conditioned matrices effectively. These solvers ensure accurate factorisation and solution of the linear systems. The solver settings were carefully fine-tuned, which involved adjusting the relative tolerances to approximately 10^{-6} to compromise accuracy and convergence efficiency. The memory allocation was adjusted to efficiently manage the computing requirements of the vast, sparsely populated matrices commonly encountered in this multiphysics issue. In addition, suitable damping and stabilization techniques were applied to address numerical instabilities. The mesh was refined, especially at the interfaces, to guarantee that the resolution was enough for capturing important events. This setup ensured resilient and precise simulations, yielding dependable insights on the efficiency of the acoustic energy collecting device.

3.2 Experiment setup of quarter wavelength resonator acoustic energy harvesting device

An experimental setup is the physical arrangement of equipment, materials, and protocols used to conduct a scientific experiment or study methodically. It enables the researcher to manipulate factors and typically includes materials and specimens under study, any instruments or sensors for observing and collecting data, equipment for controlling or adjusting testing parameters, measurement and analysis tools, data recording devices, and a physical layout that takes safety and experimental process order into account [31, 32].

This study intends to use the configuration mentioned earlier to explore the performance and viability of acoustic energy harvesting. The experiment will entail performing experiments to quantify the system's energy conversion efficiency and power output under various acoustic situations. The outcomes of this experiment will enhance the comprehension of acoustic energy collecting systems and their prospective applications across many domains. A resonator tube with dimensions equal to one-fourth of the desired acoustic wavelength was created for the experiment.

The quarter-wavelength resonator tube was constructed using a cylindrical tube made of acrylic. The tube was straight, with a backplate glued with epoxy at one end. The backplate was secured using a piezoelectric device. Electrical cables are attached to the piezoelectric material's upper and lower electrodes to measure the voltage produced. The tube resonator had an inner diameter of 10 centimetres and an exterior diameter of 110 millimetres. The QWR is equipped with two holes for inserting pressure microphones. The first hole, Mic 2, is 50 mm from the backplate. The second hole, designated as Mic 1, is located 50 mm from the entrance of the resonator tube. Both pressure microphones utilised were of the GRAS 40PH CCP model.

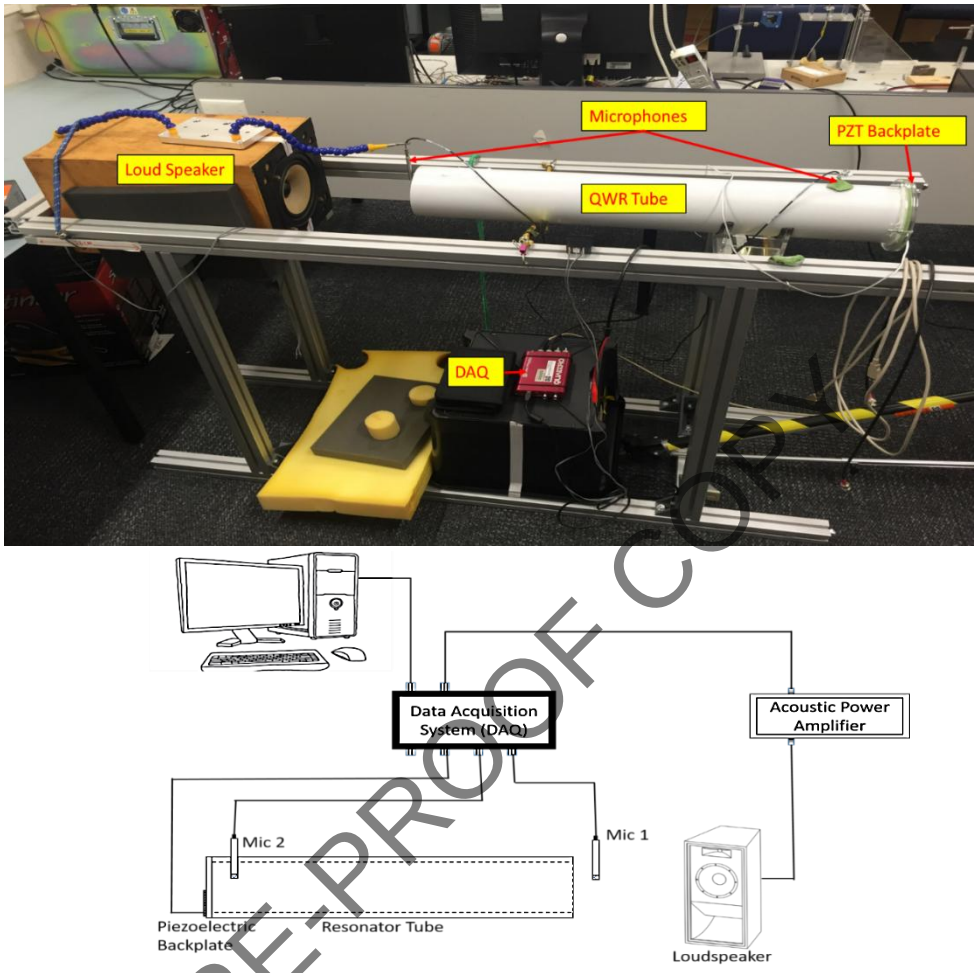

Figure 6. A quarter wavelength resonator and a flexible PZT backplate are used in the experimental setup and schematic diagram for acoustic energy collecting.

Figure 6 depicts the physical configuration and schematic representation of the experimental setup. Subsequently, the tube resonator is positioned in the trajectory of an acoustic wave emitter, such as a loudspeaker oriented at a right angle to the direction of sound wave propagation. The Signalcalc Ace Quattro, an output input data acquisition (DAQ) module, was utilised to provide the acoustic input and record the output of the AEH-QWR system. The data acquisition (DAQ) module generated a chirp signal with a frequency range of 50 to 250 Hz. This signal was amplified using a DIGITECH stereo power amplifier driver and transmitted to an 8-ohm speaker through an RS 6 12-inch bass drive unit. Mic 1 recorded the speaker's chirp signal, generating an approximate incident sound pressure of 1 Pascal (Pa). The incident acoustic wave with a pressure amplitude of 1 Pascal will travel from the loudspeaker into the straight tube of the Quarter-Wave Resonator (QWR).

A standing wave occurs when the reflected wave at the backplate interferes with the continually arriving acoustic wave. The measurement of this phenomenon will be conducted using a microphone 2. Pressure waves influence the open end and bounce back and forth within the cavity, which is one-fourth the length of a wave. This wave interaction creates a standing wave, which transfers increased vibrational energy to the piezoelectric material through acoustic resonance. The piezoelectric effect generates strain within the material, resulting in the separation of charges across its electrodes. This process converts acoustic vibrations into electrical energy. The output of the AEH system from Mic 1, Mic 2, piezoelectric, and backplate displacement will be transmitted to the data acquisition (DAQ) module and processed by specialised software for post-processing. The DAQ system was utilised to evaluate the frequency responses of different components. It prepared and measured the open-circuit output voltage produced by the backplate's lateral vibration and the microphones. In order to deliver the power output voltage, a voltage output circuit will be constructed using the strain

produced by the piezoelectric effect and connected to a variable load resistance. Each cycle will see a change in the load resistance value until the ideal power output is reached.

This experiment was conducted without using an anechoic chamber in a laboratory setting. In this experiment, the reflected wave from the surroundings significantly affected the acoustic energy-gathering apparatus. It improved the acoustic energy harvesting device's usefulness. Positive results were obtained from the experiment evaluating the feasibility of acoustic energy harvesting with a quarter-wavelength resonator and a piezoelectric backplate. The findings indicate that this configuration can efficiently convert acoustic waves into electrical energy, demonstrating significant power output and energy conversion efficiency. These results emphasise the potential of acoustic energy harvesting, especially in urban environments where sound energy is widely available. The conclusions of this study also serve to validate the accuracy of the finite element analysis used in the investigation.

4.0 RESULTS AND DISCUSSION

The results and discussion are divided into three important elements depending on the quarter-wavelength resonator with a piezoelectric backplate:

i. Total acoustic pressure inside the QWR.
ii. Open circuit voltage
iii. Power output for the QWR.

4.1 Total acoustic pressure inside the QWR with piezoelectric backplate

Acoustic energy harvesting involves converting sound waves into electrical energy. In this study, a quarter-wavelength resonator combined with a flexible PZT backplate was used as the core of the energy harvesting system. The resonator was designed based on quarter-wavelength theory to efficiently capture and amplify sound within a specific frequency range (low-frequency). The results showed that both the placement of the piezoelectric transducer and the resonator design significantly improved the system's performance and reliability. Experimental validation confirmed a strong agreement between the predicted and measured outputs. The quarter-wavelength resonator consistently demonstrated effective energy capture across various noise frequencies, highlighting the system's suitability for use in urban environments.

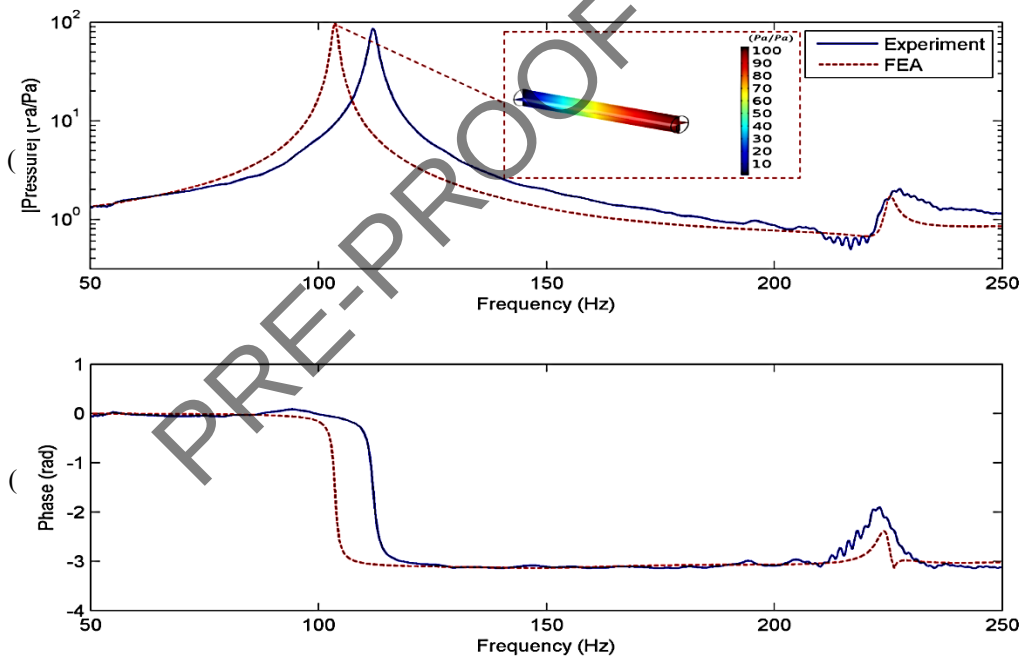

Figure 7. Acoustic pressure ratio $\left({}^{p_2}/_{p_1}\right)$ frequency response for experiment and FEA: (a) Magnitude and a small figure is a 3-D plot from FEA (b) phase

The crucial aspect of the experimental findings was the significant increase in acoustic pressure, from 1 Pa to 86 Pa, achieved by the amplification process in studying the quarter wavelength resonator. The collected data demonstrated a noteworthy rise in acoustic pressure inside the resonator, highlighting its efficient capability to trap and amplify acoustic energy. **Figure 7** displays the experimental and Finite Element Analysis (FEA) outcomes for the frequency response's magnitude and phase of the acoustic pressure ratio, $\left({}^{p_2}/_{p_1}\right)$. The FEA exhibited resonance peaks at frequencies of 104 Hz $(f_1)$and 225.5 Hz (f_2) while the experiment showed resonance peaks at frequencies of 112 Hz (f_1) and 226.75 Hz (f_2). The first resonance was primarily caused by the acoustic properties of the quarter wavelength resonator (QWR), while the second resonance was due to the structural properties of the piezoelectric backplate. The experiment proves

that the initial pressure of 1 Pa rose to 86 Pa at a frequency of 112 Hz. Similarly, the Finite Element Analysis (FEA) yielded an increase to 96 Pa at a frequency of 104 Hz. The increase in acoustic pressure clearly illustrates how the quarter-wavelength resonator efficiently captures energy from urban noise situations. The results suggest that there is great potential for using the increased acoustic pressure in real situations for a variety of energy-harvesting reasons. The resonant frequency peak of the piezoelectric backplate generated a total acoustic pressure of approximately 1.75 Pa for finite element analysis and 1.9 Pa for experimental analysis. The findings show that the flexible backplate of the resonator can maximise its standing wave and that many integrations of piezoelectric material into the backplate can be made without affecting the resonant frequency of the resonator tube. Prior researchers faced a challenge when replacing the piezoelectric component inside the resonator tube with a stiff backplate, as it caused a shift in the resonant frequency [19]. Hence, the piezoelectric backplate can be affixed to one or many piezoelectric elements to enhance power generation without causing any alterations to the resonator's resonance frequency.

The experiment and FEA showed a notable difference in the frequency response for the acoustic resonance frequency **(Figure 7).** This disparity was because the end correction of the acoustic length for both studies was different, affecting the resonator length. The theoretical equation for the quarter wavelength necessitates an effective acoustical length with respect to the actual length of the resonator. Although the theoretical Helmholtz resonator equation did not explicitly mention it, the end correction and tube length influenced the acoustic frequency, as depicted in **Figure 7**. Another factor that influenced the differences in the results was the air gap between the acoustic source and the quarter-wavelength resonator (QWR) used in the experiment. The air gap exhibits the phenomenon of uncertainty, wherein the potential for the acoustic wave to be reflected from the wall or chamber into the measurement equipment is present during initial propagation.

Meanwhile, a finite element analysis 3D plot in **Figure 7 (a)** depicted the acoustic wave transmitted in the resonator tube, which resulted in the standing wave that aroused the backplate. The resonator had its highest amplitude at the end, confirming the mode form of the initial resonance in the acoustic system. The image demonstrates that the resonance frequency of the structure was well-matched in both tests.

Table 2 presents the findings obtained from **Figure 7**, encompassing both acoustic and structural modes. The damping ratio was derived from the experiment and utilised in the finite element analysis (FEA) for validation analysis. The investigation yielded an experimental acoustic energy harvester quality factor of 61, with a damping ratio of approximately 0.0082 for one resonance frequency and approximately 0.009 for another. The findings indicated that the damping ratio significantly influenced the quarter-wavelength resonator's performance in harvesting acoustic energy. A decrease in the damping ratio caused a greater amplification of acoustic pressure in the resonator, increasing power output. In contrast, a more excellent damping ratio resulted in a drop in the amplification of acoustic pressure and consequently reduced the collected power output. Further investigation will be conducted on this parameter.

Table 2: Experiment and FEA results for both modes.

Mode	Damping ratio	Experiment		FEA		Error Percentage Natural Frequency (%)	Error Percentage Peak (%)
		Natural Frequency (Hz)	Peak (Pa/Pa)	Natural Frequency (Hz)	Peak (Pa/Pa)		
1	0.0082	112	86	104	96	7.7	10.4
2	0.009	226.75	1.9	225.5	1.75	0.6	8.5

During the error analysis in **Table 2,** it became clear that there were substantial disparities between the findings derived from the experimental analysis and the finite element analysis. This discrepancy suggests a possible divergence between the theoretical assumptions and the actual behaviour of the studied system. The observed inconsistencies may have been greatly influenced by the material properties, boundary conditions, and modelling assumptions [32]. The natural frequency value for both studies shows an error percentage of not more than 10%, which is acceptable for the acoustic energy harvesting device. Even though in the experiment, the reflected wave in the surroundings can affect the harvesting process, it shows not much difference in the frequency value compared to the finite element analysis.

In summary, fully coupled finite element analysis using COMSOL for acoustic energy harvesting with a quarter-wavelength resonator and piezoelectric backplate provides a more accurate and realistic model by accounting for all interactions between the involved physics domains simultaneously. This leads to better predictive capability and alignment with experimental results. However, it is computationally intensive and requires a complex setup [33]. On the other hand, decoupled analysis offers a more straightforward and faster approach with lower computational demands, but at the cost of reduced interaction accuracy and the potential introduction of inconsistencies

4.2 Open circuit voltage for QWR with piezoelectric backplate

The experimental analysis of the quarter-wavelength resonator with a piezoelectric backplate yielded some exciting results. The open circuit voltage highly depended on the excitation frequency, with a clear peak at the resonant frequency. These results confirm the expected behaviour of the resonator and validate its design. In addition to the experimental analysis, finite element analysis was performed to investigate further the open circuit voltage of the quarter wavelength resonator with a piezoelectric backplate. The finite element analysis results showed excellent agreement with the

experimental findings, providing a comprehensive understanding of the device's behaviour. **Figure 8** shows the frequency response of the ratio voltage open circuit to pressure at the inlet, $^{OCV}/_{p_1}$ for experiment and FE analysis. The acoustic standing wave inside the tube caused the acoustic particle velocity at the end of the backplate, which was embedded with a piezoelectric patch excited at the same displacement. This excitation of the piezoelectric element at the backplate generated a significant amount of voltage. The output voltage obtained from the piezoelectric without any resistive load was known as a voltage open circuit (VOC).

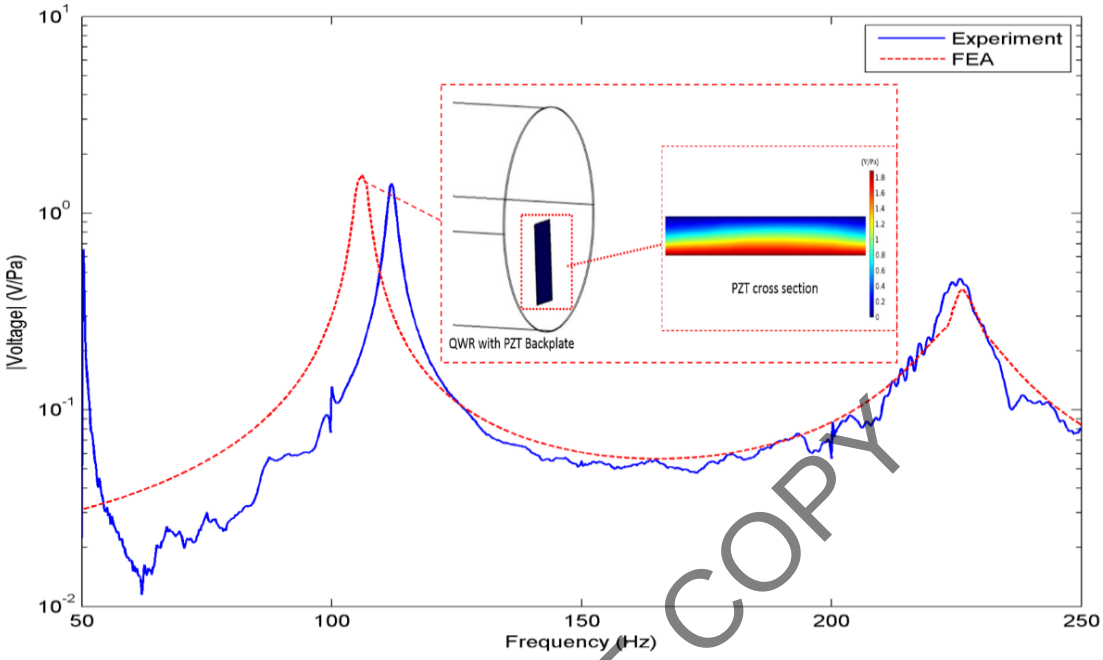

Figure 8. Frequency response of $(^{OCV}/_{p_1})$.for experiment and FEA. Small figure FEA 3-D plot.

The total output voltage open circuit for simulation was around 1.44 V/Pa (at 104 Hz) and 0.41 V/Pa at 225.5 Hz. In comparison, the experiment showed 1.41 V/Pa at 112 Hz and 0.44 V/Pa (at 226.75 Hz). By comparing the experimental and finite element analysis results, it was found that both methods yielded similar results for the natural frequency of both the annular and circular plates, with a percentage error of less than 10%. The concurrence between experimental and simulation outcomes validated the finite element model's capability to faithfully represent the resonator's intricate mechanical and electrical dynamics. The examination demonstrated that the resonator's standing wave of acoustic pressure stimulated the piezoelectric backplate, generating an open-circuit voltage. The resonance behaviour observed in the experimental analysis was further validated by the fact that this effect was most pronounced at the resonant frequency. The observed correlation between the generation of open circuit voltage and the standing wave of acoustic pressure was in accordance with the theoretical predictions. As mentioned earlier, the discovery validates the piezoelectric backplate's efficacy in transforming acoustic energy into electrical energy and underscores the criticality of resonant frequency in maximising the device's functionality.

Figure 8 also displays a three-dimensional plot of FEA that focuses on the open-circuit voltage generated by the piezoelectric plate. Based on the PZT cross-section view, the plot legend indicates that the blue region is connected to the ground node, while the red region is connected to the terminal node. This FEA establishes a boundary condition for linking with external circuits and transmission lines or applying a specified voltage or charge. A thorough finite element analysis obtained a deeper understanding of the device's vibration patterns and electric potential distribution, providing valuable insights into the fundamental physics that drive the energy harvesting process. Through the simulation of the acoustic energy harvesting process, the finite element analysis yielded essential data on the relationship between the open circuit voltage and the excitation frequency, as well as the design parameters of the piezoelectric backplate.

Nevertheless, although the experimental and simulation outcomes present convincing evidence for the effectiveness of the resonator design, it is vital to consider any potential limitations and alternative explanations for the observed results. Based on empirical evidence and computer modelling, it has been observed that the relationship between open-circuit voltage and excitation frequency can be affected by various factors beyond the resonator's design. Overall, the experimental and finite element analysis results suggest that the quarter-wavelength resonator generates an open-circuit voltage by exciting the piezoelectric backplate with acoustic pressure standing waves.

4.3 Power output for the QWR with piezoelectric backplate

The experimental and finite element analyses offer valuable insights into the electricity generation process in acoustic energy harvesting. Specifically, they focus on the voltage-closed circuit and the utilisation of a quarter wavelength resonator with a piezoelectric backplate. The relationship between the open-circuit voltage and excitation frequency, as

supported by experimental and simulation results, aligns with theoretical expectations, showcasing the effectiveness of the resonator design. To delve deeper into the study of the quarter wavelength resonator with a flexible lead zirconate titanate backplate, the next course of action involves exploring the power generation capabilities of the resonator under various resistive loads. This analysis will offer valuable insights into the device's performance under different electrical loads, providing crucial information for practical applications in energy harvesting systems.

This study will connect the piezoelectric element to the resistive load to obtain the power output from the open circuit voltage (OCV) and AEH system. The power output can be acquired by adding several resistive loads at one node and generating an output voltage with optimum load résistance (VL). From the measured variable load resistance, the total power was obtained by $^{VL^2}/_{R_{optimum}}$ for 104 Hz and 225.5 Hz for simulation, and the resonance frequency from the experiment was 112 Hz and 226.75 Hz. **Figure 9** shows the power generated by QWR with a flexible PZT backplate at different resistive loads. By systematically evaluating the power output across various resistive loads, the AEH system comprehensively understands the resonator's behaviour and ability to generate electricity efficiently. This investigation will also validate the effectiveness of the resonator design in delivering practical and usable power output, further solidifying its potential for real-world applications. The power generated by the QWR with the flexible PZT backplate at different resistive loads will be crucial in determining the optimal operating conditions for maximising power extraction while considering the requirements of specific energy harvesting applications. Additionally, this analysis will provide essential data for optimising the electrical circuitry and load-matching strategies to achieve maximum power transfer efficiency from the resonator.

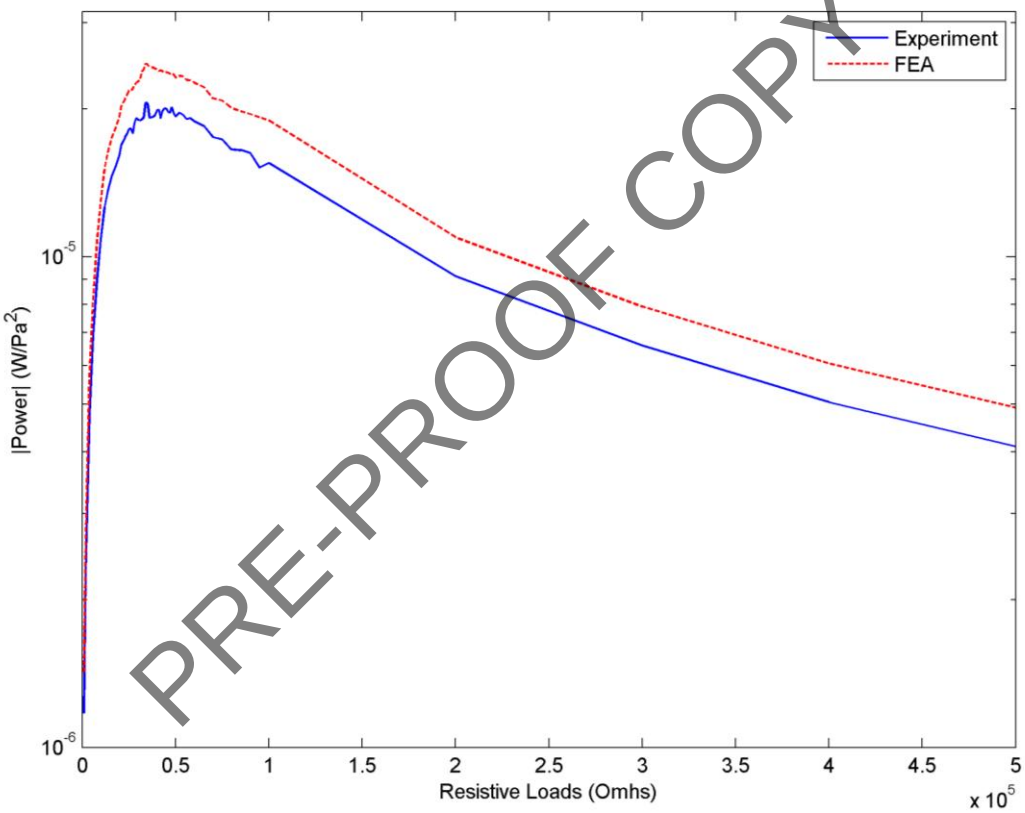

Figure 9. Experiment and FEA result for the output power of the AEHs for different resistive loads.

The study's findings indicate that a load resistance value of 36 kΩ yielded the best output power value for both resonance frequencies. Based on the data, the power output of the AEH-QWR system decreased as the resistive loads increased beyond the optimal point. The QWR demonstrated its power with a flexible PZT backplate, showcasing its ability to handle various resistive loads.

Through FEA simulation, the optimal power was determined to be 24.2 $\mu W/Pa^2$ at 106 Hz,. In comparison,the experiment yielded a slightly lower value of 20.2 $\mu W/Pa^2$ at 112 Hz. The findings of this study will enhance our knowledge of how energy is converted. However, they will also provide valuable insights for incorporating the QWR with flexible PZT backplates into energy harvesting systems. The experimental and finite element analysis results show the practicality and efficiency of utilising a quarter wavelength resonator with a piezoelectric.

Based on the analysis conducted in the previous stage, it has been determined that the ideal load resistance for the first resonance is 36 kΩ. This discovery is essential in determining the optimal operating conditions for maximising power extraction from the quarter wavelength resonator with the flexible PZT backplate. When the load resistance is adjusted to 36 kΩ, the resonator proves its electricity efficiency, further confirming its practical use in energy harvesting systems. A thorough understanding of the resonator's behaviour at this particular load resistance is crucial for maximising power

output and ensuring optimal device performance. This analysis will offer valuable insights into the resonator's response to electrical loads, helping to develop customised strategies for maximising power extraction while ensuring operational efficiency. Examining the voltage closed circuit behaviour of the resonator at different resistive loads will provide insights into its power generation efficiency under various operating conditions. This investigation will help improve the resonator's design and provide insights for enhancing power generation and voltage output. A clear grasp of how power generation fluctuates with frequency when faced with different resistive loads is essential to determine the resonator's ideal operating frequency range and optimise its power extraction potential.

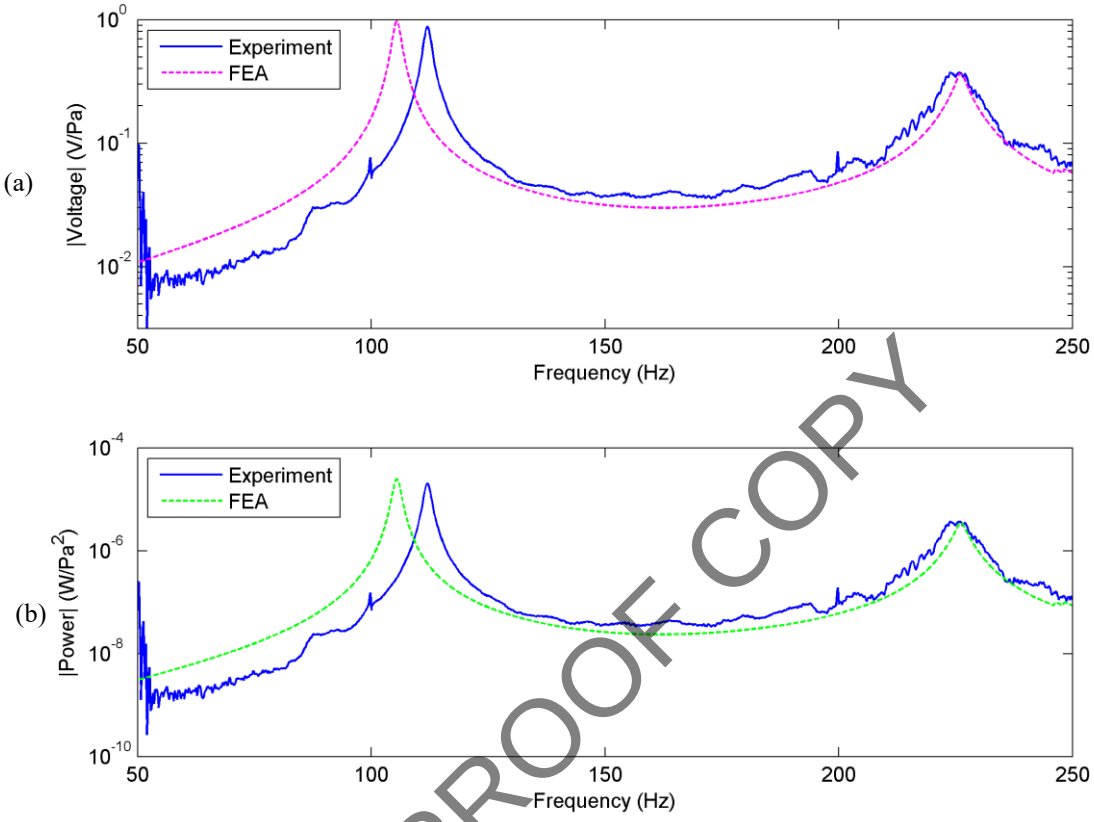

Figure 10. Frequency response at optimum resistive load for experiment and FEA: (a) voltage with load resistance $\left({}^{VL}/_{p_1}\right)$ (b) power output $\left({}^{Power}/_{p_1{}^2}\right)$

At optimum load resistance and pressure at the inlet, p_1 **Figure 10 (a)** illustrates the voltage closed-circuit frequency response, while **Figure 10 (b)** illustrates the power frequency response at the same pressure. The QWR, equipped with a piezoelectric backplate, produced the highest power output for FEA (Finite Element Analysis) at a frequency of 106 Hz measuring 24.2 $\mu W/Pa^2$ This result closely aligned with the experimental finding of 20.2 $\mu W/Pa^2$ at a frequency of 112 Hz. The resonator's power production capabilities are clearly and consistently demonstrated. The power output of the quarter-wavelength resonator with a piezoelectric backplate has been effectively confirmed through experimental and finite element analysis. This mechanism confirms its ability to capture energy. The correlation between the empirical results and Finite Element Analysis (FEA) forecasts bolsters the dependability and precision of the resonator's power-generating capabilities.

The power output and closed voltage circuit exhibit two amplitude peaks in their frequency response. Figure 10 demonstrates that both the experimental and finite element analyses validate the power output of the quarter wavelength resonator with a piezoelectric backplate, thereby highlighting its capacity to capture and utilize energy. The comparison of experimental results with finite element analysis (FEA) predictions further enhances confidence in the dependability and accuracy of the resonator's power-generating capabilities. By conducting a thorough validation process, the agreement between the experimental and Finite Element Analysis (FEA) results will confirm the accuracy of the analytical models and instil confidence in the practical use of the quarter-wavelength resonator with the PZT backplate for energy harvesting applications.

5.0 CONCLUSIONS

In conclusion, the research has demonstrated the potential of quarter-wavelength-resonator acoustic energy harvesting as a viable method for capturing urban noise and converting it into usable energy. The fully coupled modelling and

experimental validation have provided valuable insights into the behaviour and performance of the energy harvesting system. A fully-couple finite element analysis shows an advantage in containing all the necessary degrees of freedom. Although the established software can simulate the analysis, it has limitations with long simulation time and computer specification constraints. Considering the mesh and in specific particular applications, it is essential to access the specific boundary condition and which kind of dynamic system was analysed. Then, a fully coupled analysis can be obtained, and simulation time can be reduced. The results of a fully coupled simulation analysis compared to the experiment of an acoustic energy harvesting mechanism using a quarter wavelength resonator (QWR) tube with a piezoelectric back plate using dedicated software were conducted, and the results were produced. This QWR energy harvesting mechanism harvested acoustic energy at a low frequency (around 70 Hz ~ 130 Hz) with an incident wave of 90 dB pressure. The piezoelectric back plate generated a voltage open circuit of around 1.88 V/Pa (at 106.5 Hz) and 0.75 V/Pa at 224 Hz compared to the experimental 1.73 V/Pa at 112 Hz and 0.36 V/Pa (at 228 Hz). Meanwhile, the power dissipated in the resistor for the experimental was 20.4 $\mu W/Pa^2$ at 112 Hz and 3.6 $\mu W/Pa^2$, whereas the simulation reaches a maximum of 24.2 $\mu W/Pa^2$ at 106.5 Hz and 6.87 $\mu W/Pa^2$ at 228 Hz. The frequency response results were based on the acoustic pressure of Mic1, which was the element resonator passive noise attenuation that occurred at the inlet of the resonator.

The main findings of this preliminary study indicate that the quarter-wavelength-resonator can efficiently capture and convert urban noise into electrical energy, with the experimental results closely matching the predictions of the coupled model. Additionally, the study emphasises the significance of considering the intricate relationships between the resonator parameter, acoustic source, converter mechanism and electrical circuit when designing and optimising energy harvesting systems. By thoroughly understanding these relationships, future research can enhance and refine the efficiency of quarter-wavelength-resonator acoustic energy harvesting technology. The study also shows that comparing fully coupled finite element analysis (FEA) using COMSOL for acoustic energy harvesting with a quarter-wavelength resonator and piezoelectric backplate against decoupled analysis highlights distinct advantages and considerations for each approach. In fully coupled FEA, all relevant physical interactions, such as acoustic waves, structural deformations, and piezoelectric responses, are solved simultaneously, providing a comprehensive and accurate representation of the energy harvesting system. This approach is particularly effective at capturing intricate interactions, such as the process by which acoustic waves cause structural vibrations that subsequently provide electrical output via the piezoelectric effect. This comprehensive method improves the ability to forecast outcomes accurately and provides an in-depth understanding of how systems behave in different circumstances. On the other hand, decoupled analysis refers to addressing each physical domain separately and in a certain order, which can make the setup easier and decrease the computational requirements. Nevertheless, decoupling can result in mistakes when representing the effects of strong coupling and nonlinear interactions across different domains. This compromises the accuracy and reliability of the conclusions, particularly in complex systems. Hence, the decision to use either completely coupled or decoupled analysis relies on the particular objectives of the study, including the level of accuracy needed, available computer resources, and the characteristics of the physical interactions within the energy harvesting system.

Overall, the findings of this research paper contribute to the growing body of knowledge in energy harvesting and sustainable urban development. The successful coupling of theoretical modelling and experimental validation sets a strong foundation for further advancements in applying acoustic energy harvesting technology. Additional research and development in this area have the potential to make meaningful contributions to energy sustainability in urban environments.

6.0 CONFLICT OF INTEREST

The authors declare that they have no known competing interests that could have influenced this article.

7.0 AUTHORS CONTRIBUTION

MHM: Investigation, Validation, Methodology, Formal Analysis, Writing – Original Draft, Funding Acquisition.
MSMS: Investigation, Formal Analysis, Data Curation, Supervision, Writing – Review & Editing
MFH: Conceptualization, Writing – Review & Editing, Supervision, Funding Acquisition, Project Administration
LHT: Conceptualization, Supervision, Writing – Review & Editing, visualisation

8.0 ACKNOWLEDGEMENTS

The authors would like to express their gratitude to the Advanced Structural Integrity and Vibration Research Group (ASIVR) at Universiti Malaysia Pahang Al-Sultan Abdullah for providing laboratory facilities and financial assistance under project grant number RDU230339.

9.0 REFERENCES

[1] F. J. Fahy, "Sound and Structural Vibration: Radiation, Transmission and Response", 2nd ed. Amsterdam, Netherlands: Elsevier, 2007.

[2] S. Saadon and O. Sidek, "A review of vibration-based MEMS piezoelectric energy harvesters," Energy Convers. Manag, vol. 52, no. 1, pp. 500–504, Jan. 2011.

[3] F. Liu et al., "A multiple degree of freedom electromechanical Helmholtz resonator," J. Acoust. Soc. Am., vol. 122, no. 1, pp. 291–301, Jul. 2007.

[4] K. Ma et al., "Metamaterial and Helmholtz coupled resonator for high-density acoustic energy harvesting," Nano Energy, vol. 82, p. 105693, Sep. 2021.

[5] M. Yuan et al., "Joint acoustic energy harvesting and noise suppression using deep-subwavelength acoustic device," Smart Mater. Struct., vol. 29, no. 3, p. 035012, Mar. 2020.

[6] B. Li et al., "Harvesting low-frequency acoustic energy using quarter-wavelength straight-tube acoustic resonator," Appl. Acoust., vol. 74, no. 11, pp. 1271–1278, Nov. 2013.

[7] X. Ji et al., "Enhanced quarter spherical acoustic energy harvester based on dual Helmholtz resonators," Sensors, vol. 20, no. 24, p. 7275, Dec. 2020.

[8] A. Yang et al., "Enhanced acoustic energy harvesting using coupled resonance structure of sonic crystal and Helmholtz resonator," Appl. Phys. Express, vol. 6, no. 12, p. 127101, Dec. 2013.

[9] M. E. Amorim et al., "A simple experiment to explore standing waves in a flexible corrugated sound tube," Phys. Teach., vol. 49, no. 6, pp. 360–362, Sep. 2011.

[10] C. Field and F. Fricke, "Theory and applications of quarter-wave resonators: A prelude to their use for attenuating noise entering buildings through ventilation openings," Appl. Acoust., vol. 53, no. 1–3, pp. 117–132, Jan. 1998.

[11] S. B. Horowitz, "Development of a MEMS-based acoustic energy harvester," M.S. thesis, Univ. of Florida, Gainesville, FL, USA, 2004.

[12] F. Liu, "A Tunable Electromechanical Helmholtz Resonator," presented at the 9th AIAA/CEAS Aeroacoustics Conf. and Exhibit, Hilton Head, SC, USA, 2003, AIAA Paper 2003.

[13] I. K. Kim and Y. Y. Kim, "Wireless frequency-tuned generation and measurement of torsional waves using magnetostrictive nickel gratings in cylinders," Sens. Actuators A Phys., vol. 126, no. 1, pp. 73–77, Jan. 2006.

[14] S. Matova et al., "Harvesting energy from airflow with a micromachined piezoelectric harvester inside a Helmholtz resonator," J. Micromech. Microeng., vol. 21, no. 10, p. 104001, Oct. 2011.

[15] M. Yuan et al., "An efficient low-frequency acoustic energy harvester," Sens. Actuators A Phys., vol. 264, pp. 84–89, Apr. 2017.

[16] D. Li et al., "Design of tunable low-frequency acoustic energy harvesting barrier for subway tunnel based on an optimized Helmholtz resonator and a PZT circular plate," Energy Rep., vol. 8, pp. 8108–8123, Nov. 2022.

[17] B. Li, J. H. You, and Y.-J. Kim, "Low frequency acoustic energy harvesting using PZT piezoelectric plates in a straight tube resonator," Smart Mater. Struct., vol. 22, no. 5, p. 055013, May 2013.

[18] B. Li and J. H. You, "Simulation of acoustic energy harvesting using piezoelectric plates in a quarter-wavelength straight-tube resonator," presented at the COMSOL Conf., Boston, MA, USA, 2012.

[19] B. Li and J. H. You, "Enhanced output power by eigenfrequency shift in acoustic energy harvester," in Proc. SPIE Smart Struct. Mater., 2014.

[20] B. Li and J. H. You, "Experimental study on self-powered synchronized switch harvesting on inductor circuits for multiple piezoelectric plates in acoustic energy harvesting," J. Intell. Mater. Syst. Struct., vol. 26, no. 13, pp. 1646–1655, Sep. 2015.

[21] H. Xiao et al., "Metamaterial based piezoelectric acoustic energy harvesting: Electromechanical coupled modeling and experimental validation," Mech. Syst. Signal Process., vol. 185, p. 109808, Feb. 2023.

[22] P. Gothwal and A. Kumar, "Comparative analysis of piezo energy harvester optimization techniques: A comprehensive review," J. Adv. Res. Appl. Sci. Eng. Technol., vol. 49, no. 1, pp. 211–226, Jul. 2024, doi: 10.37934/araset.49.1.211226.

[23] M. Alshahrani, R. A. Dungca, and S. Alam, "Acoustic impedance matching for enhanced energy harvesting in resonator-based devices," IEEE Sens. J., vol. 24, no. 2, pp. 1672–1680, Jan. 2024, doi: 10.1109/JSEN.2023.3321150.

[24] M. S. Islam, T. Rahman, and Y. Zhu, "Hybrid analytical-FEM modelling for low-frequency acoustic energy harvesters," Appl. Acoust., vol. 212, p. 109984, Mar. 2025, doi: 10.1016/j.apacoust.2025.109984.

[25] H.-B. Fang et al., "Fabrication and performance of MEMS-based piezoelectric power generator for vibration energy harvesting," Microelectron. J., vol. 37, no. 11, pp. 1280–1284, Nov. 2006.

[26] S. Kim et al., "Gradient-index phononic crystal and Helmholtz resonator coupled structure for high-performance acoustic energy harvesting," Nano Energy, vol. 101, p. 107544, Sep. 2022.

[27] P. M. Morse and K. U. Ingard, Theoretical Acoustics. Princeton, NJ, USA: Princeton Univ. Press, 1986.

[28] A. Soto-Nicolas, "Measurements on quarter-wavelength tubes and Helmholtz resonators," J. Acoust. Soc. Am., vol. 123, no. 5, p. 3842, May 2008.

[29] C. H. Sohn and J. H. Park, "A comparative study on acoustic damping induced by half-wave, quarter-wave, and Helmholtz resonators," Aerosp. Sci. Technol., vol. 15, no. 8, pp. 606–614, Dec. 2011.

[30] J. H. Park and C. H. Sohn, "On optimal design of half-wave resonators for acoustic damping in an enclosure," J. Sound Vib., vol. 319, no. 3–5, pp. 807–821, Jan. 2009.

[31] F. J. Fahy, "Foundations of Engineering Acoustics". Amsterdam, Netherlands: Elsevier, 2000.

[32] M. H. Mansor, M. S. M. Sani, and M. F. Hassan, "Eigenfrequency shift of piezoelectric backplate in vibro-acoustic energy harvesting," Int. J. Automot. Mech. Eng., vol. 20, no. 4, pp. 10850–10861, 2023.

[33] S. Ereiz, I. Duvnjak, and J. F. Jiménez-Alonso, "Review of finite element model updating methods for structural applications," Structures, Elsevier, vol. 36, pp. 895–913, 2022.